

An Infrared Study of CO Adsorption on Reduced and Oxidized Ru/SiO₂

G. H. YOKOMIZO, C. LOUIS,¹ AND A. T. BELL

Center for Advanced Materials, Lawrence Berkeley Laboratory, and Department of Chemical Engineering, University of California, Berkeley, California 94720

Received January 19, 1989; revised April 4, 1989

Three infrared bands are observed for CO adsorbed on Ru/SiO₂. The two highest frequency bands are assigned to the A₁ and E stretching modes of tricarbonyl species. On a reduced sample, the tricarbonyl species are associated with Ru ions bonded directly to the support. Such structures are produced by corrosive chemisorption of CO on Ru crystallites [Ru₃ + 2 SiOH + 3 CO = (SiO)₂Ru(CO)₃ + H₂]. A separate set of tricarbonyl species is observed on partially oxidized samples of Ru/SiO₂. In this case, the partially oxidized sites occur on the surface of the Ru particles. The lowest frequency band is assigned to the C-O stretch of linearly adsorbed CO on Ru particles. Evidence is also found for linearly adsorbed CO on partially oxidized Ru sites. © 1989

Academic Press, Inc.

INTRODUCTION

The chemisorption of CO on silica-supported Ru has been studied extensively by infrared spectroscopy (1-10). General agreement exists on the presence of up to three infrared bands and the position of these bands. Although there is consensus on the assignment of the low-frequency band (LF) at $2040 \pm 10 \text{ cm}^{-1}$ to linearly adsorbed CO on metallic Ru, there is disagreement over the assignment of the two high-frequency bands at (HF₁) $2140 \pm 10 \text{ cm}^{-1}$ and (HF₂) $2080 \pm 10 \text{ cm}^{-1}$. The observation of a constant ratio of the intensities of the two high-frequency bands with changing CO coverage has led several investigators to attribute the pair of HF bands to a dicarbonyl species (4, 5, 8). By contrast, other investigators have noted a change in the ratio of intensities of the HF bands and have assigned the individual HF bands to linear or multicarbonyl species (3, 9). The increase in intensity of the HF bands with oxidation of the catalyst has led

several authors to conclude that the adsorption sites associated with these bands are partially or completely oxidized (3, 4, 9). Although a difference in the positions of the HF bands for CO adsorbed on reduced and oxidized samples has been observed, only Brown and Gonzalez (3) have attempted to account for this difference, suggesting that it may be due to an electronic effect.

This paper presents the results of an infrared study of CO adsorbed on Ru/SiO₂. The objectives of this study were to elucidate the mode of CO adsorption corresponding to the HF bands, to quantify the amounts of CO associated with the LF and HF bands, and to identify the nature of the sites involved in CO chemisorption on reduced and oxidized Ru surfaces.

EXPERIMENTAL

The infrared cell used for these studies consisted of two MDC Vacuum Products miniconflat sapphire viewports (VP-075S) bolted to a machined, double-sided miniconflat flange (MDC FD-133000), which served as the sample holder. The cell was heated by Hotwatt glasrope (GR30-24) heaters connected to an Action Instruments power supply (MDL 3231-202, MDL 3020-

¹ Present address: Laboratoire de Réactivité de Surface et Structure, Université Paris VI, 4 place Jussieu, 75252 Paris Cédex 05, France.

101). The temperature inside the reactor was measured with a thermocouple placed in the gas flow close to the catalyst sample and was maintained constant by an Omega CN 2000 temperature controller connected to the heater power supply.

Infrared spectra were obtained using a Digilab FTS-15/80 Fourier-transform infrared spectrometer equipped with a narrow band HgCdTe detector. Interferograms were collected at the rate of about one every 2 s and then transformed to obtain spectra with 2-cm^{-1} resolution. A spectrum of the reduced catalyst disk taken at the same temperature as that of the sample spectrum was used as the background reference. The background spectrum was used to calculate an absorbance spectrum for the adsorbate. Infrared peaks were deconvoluted by fitting each peak to the sum of Lorentzian and Gaussian lineshapes.

H₂, CO, and He were supplied to the infrared cell from a gas manifold and the cell effluent was analyzed by an EAI 250B quadrupole mass spectrometer. Details of this portion of the apparatus are given in Ref. (11). UHP hydrogen from Matheson was purified by passage through a Deoxo purifier (Engelhard) and molecular sieves (Linde 13 \times) cooled in dry ice. Helium obtained from the Lawrence Berkeley Laboratory was purified by passage through Oxy-Absorbent (Alltech Associates) and molecular sieves cooled in dry ice. UHP carbon monoxide from Matheson was purified of iron carbonyls by passage through a copper tube packed with glass beads and heated to 473 K. Further purification was accomplished by passage through Ascarite and molecular-sieve-cooled in dry ice. Isotopically labeled 99% ¹³CO was obtained from Isotec and used without further purification.

A 3.52% Ru/SiO₂ catalyst was prepared by incipient wetness impregnation of Cab-O-Sil HS-5 (Cabot) with an aqueous solution of Ru(NO₃)₃ (Engelhard) (1 cm³ solution per g of support). The impregnated support was dried in air at 373 K overnight.

The catalyst was ground and 40 mg was pressed into a 1.55-cm-diameter self-supporting disk. The catalyst disk was placed in the infrared cell and then reduced in flowing hydrogen. The reduction temperature was increased at 0.2 K/s from room temperature to 673 K and then maintained at this temperature for 2 h. The sample was then outgassed for 30 min at 673 K in flowing He to remove chemisorbed hydrogen. Temperature-programmed desorption showed that H₂ completely desorbs by 420 K. Following reduction, the catalyst temperature was lowered to room temperature and the desired adsorbate was introduced. CO was typically adsorbed by flowing 40 Torr of CO over the sample for 15 min at room temperature. The gas-phase CO was removed by flushing the sample with He for 5 min. A dispersion of 33% was measured by CO chemisorption following reduction in flowing H₂ at 673 K. The stoichiometry of CO to Ru was determined using the results of this study. Ru weight loading was determined by X-ray fluorescence.

RESULTS

A representative spectrum of ¹²CO adsorbed at 298 K on reduced Ru/SiO₂ is given in Fig. 1. Three peaks are observed at 2144 (HF₁), 2082 (HF₂), and 2047 cm⁻¹ (LF). The LF band comprises 90% of the spectral area. The ratio of the area of HF₁ band to that of the HF₂ band is approximately 0.5. Passage of a flow of He over the catalyst results in a slight decrease in the intensity and shift of the LF band to lower frequency, as shown in Fig. 1. Neither of the HF bands is affected by flushing the cell with He. Adsorption of ¹³CO produces a spectrum identical in shape to that shown in Fig. 1, but shifted downscale by approximately 50 cm⁻¹.

To complement the studies performed using fully reduced samples, spectra were recorded on samples which had been intentionally oxidized by exposure to 160 Torr O₂ at 298 K for 5 min. The total uptake of ¹²CO on the partially oxidized sample was

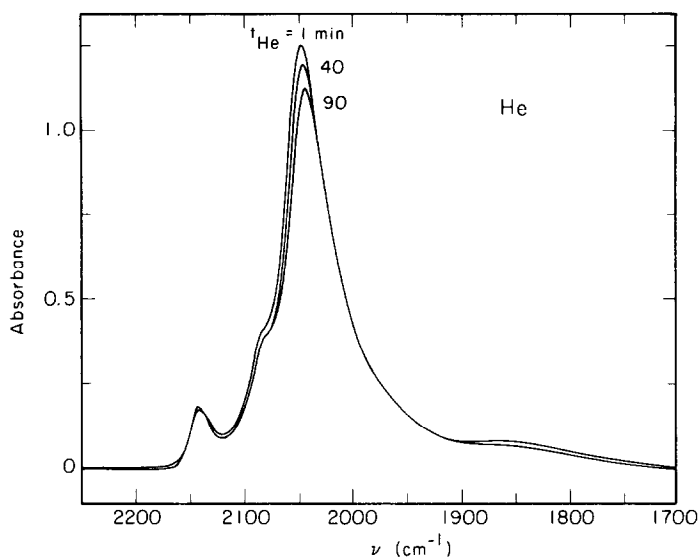


FIG. 1. Effect of He outgassing at 298 K on the band intensity for ¹²CO adsorbed on reduced Ru/SiO₂.

half of that on the reduced sample. The spectrum of ¹²CO adsorbed on partially oxidized Ru/SiO₂ is shown in Fig. 2. Three bands are seen at 2136, 2080, and 2032 cm⁻¹. The intensities of the HF bands are greater than those for the reduced sample,

but the intensity of the LF band is significantly smaller and accounts for less than 65% of the total spectral area. It is also noted that the ratio of the intensities of HF₁/HF₂ is approximately 0.5. Upon flushing with He, the LF band decreases signifi-

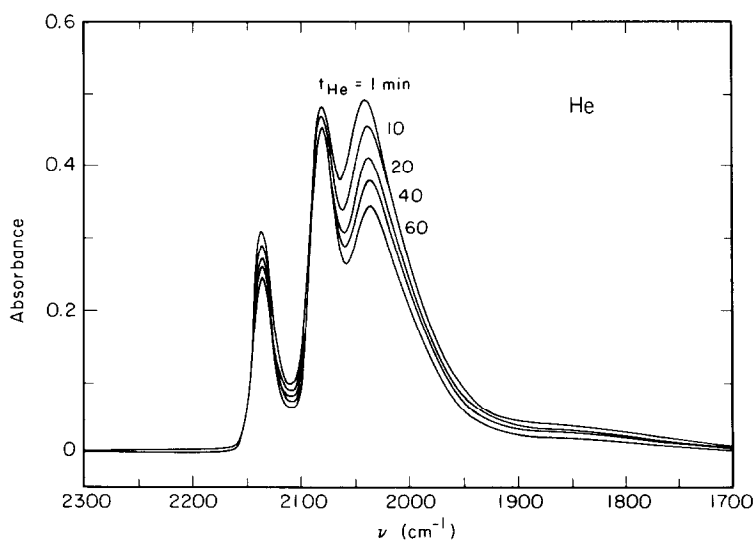


FIG. 2. Effect of He outgassing at 298 K on the band intensity for ¹²CO adsorbed on oxidized Ru/SiO₂.

TABLE I
Integrated Band Intensities Observed During He
Flushing of Oxidized Ru/SiO₂^a

Min in He	HF ₁	HF ₂	LF	HF ₁ /HF ₂
1	5.9	13.5	—	0.43
5	5.6	13.5	41.2	0.42
10	5.4	13.8	39.9	0.38
20	5.3	14.3	35.8	0.37
40	5.2	15.1	34.6	0.34

^a Arbitrary units.

cantly and to a lesser extent so does the HF₁ band, but the intensity of the HF₂ band increases as shown in Table 1.

In an effort to distinguish between the HF bands on an oxidized versus a reduced catalyst, spectra were recorded after pulsing O₂ over ¹³CO adsorbed on the reduced catalyst. Figure 3 shows that the O₂ pulses (4 μmol O₂/pulse) seem to have no effect on the intensity of the HF₁ band present on the reduced surface and that a new HF band develops at a frequency 12 cm⁻¹ lower than

that of the HF₁ band initially present. It is also seen that passage O₂ pulses over the catalyst reduces the intensity of the LF band, but increases the intensity of the HF₂ band. Passage of 10 oxygen pulses over a reduced catalyst initially covered with 120 μmol of CO/g generates 45 μmol of CO₂ and 10 μmol of CO. The ratio of the intensities HF₁/HF₂ after pulsing O₂ is four to five times less than the ratio measured when the catalyst is oxidized before CO adsorption. Figure 4 shows that ¹³CO readsorption after O₂ pulsing over the reduced catalyst initially covered with ¹³CO increases the ratio of the HF₁/HF₂ band to about 0.5. It is also noted that the positions of the HF₁ and HF₂ bands remain fixed.

The effect of increasing ¹³CO coverage on the spectra of the reduced catalysts is given in Fig. 5. At low coverage, only the LF band is present at 1981 cm⁻¹. With increasing coverage, the LF band shifts towards 1995 cm⁻¹ and two HF bands appear at 2095 and 2035 cm⁻¹. The positions of these latter features are independent of coverage. On an oxidized surface, both the

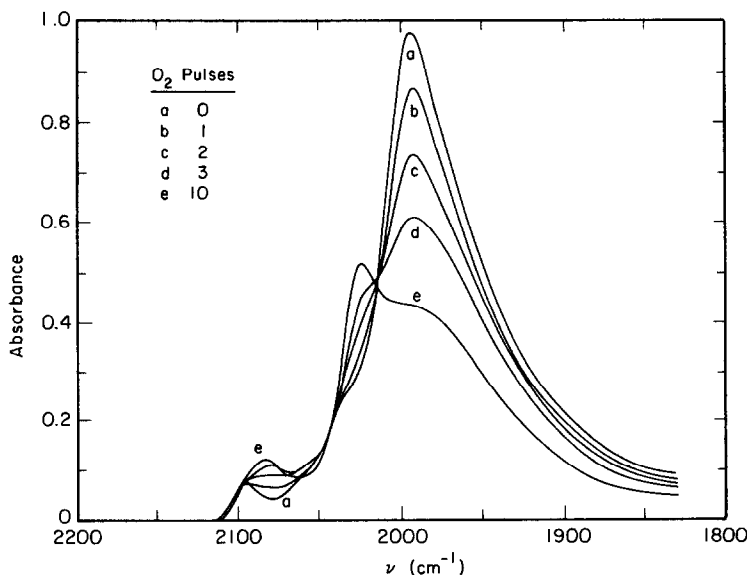


FIG. 3. Effect of 4 μmol oxygen pulses on the spectrum of ¹³CO adsorbed on reduced Ru/SiO₂: (a) ¹³CO adsorbed on reduced catalyst, (b) after 1 O₂ pulse, (c) after 2 pulses, (d) after 3 pulses, (e) after 10 pulses.

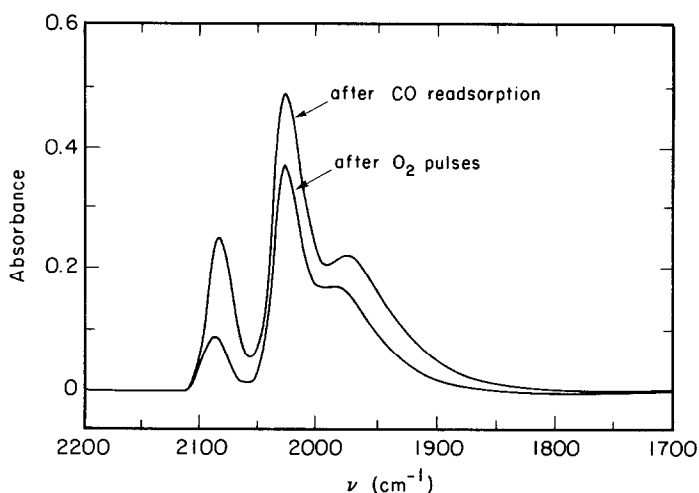


FIG. 4. Spectra of adsorbed ¹³CO: (1) after pulsing oxygen; (2) following (1) and readsorption of ¹³CO.

HF₂ band and the LF band are formed at low ¹²CO coverage as shown in Fig. 6. With increasing ¹²CO coverage, the HF₁ band appears and the intensity of the HF₂ band grows relative to that of the LF band. It is noted, however, that neither of the HF

bands exhibits a shift in position with increasing CO coverage.

Spectra recorded of ¹²CO adsorbed on a reduced sample before and after isotopic exchange with gaseous ¹³CO show that only the LF band exchanges at 298 K and that

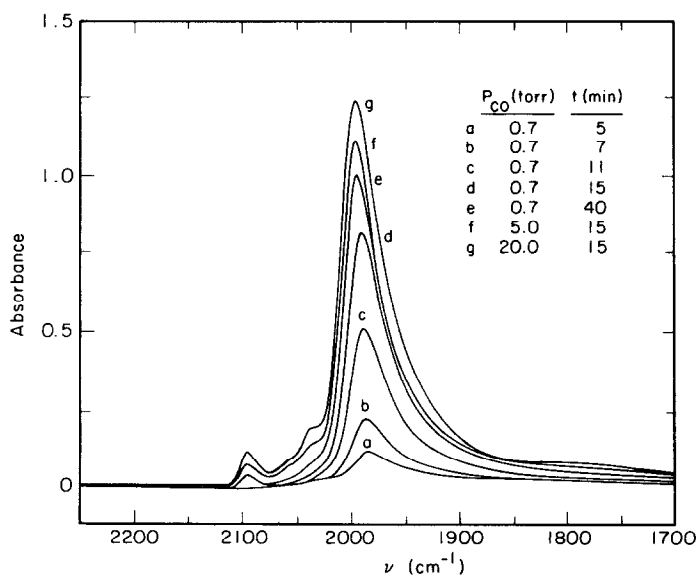


FIG. 5. Spectra of adsorbed ¹³CO on reduced Ru/SiO₂ taken as a function of increasing ¹³CO pressures: (a) 0.7 Torr, 5 min; (b) 0.7 Torr, 7 min; (c) 0.7 Torr, 11 min; (d) 0.7 Torr, 15 min; (e) 0.7 Torr, 40 min; (f) 5 Torr, 15 min; (g) 20 Torr, 15 min.

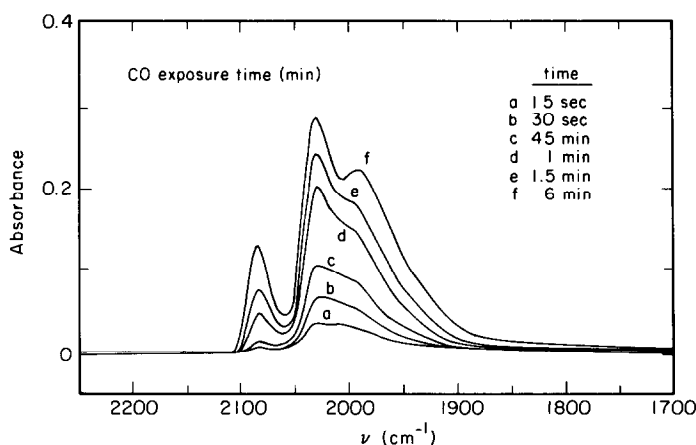


FIG. 6. Spectra of adsorbed ^{13}CO on oxidized Ru/SiO_2 taken as a function of increasing time of exposure to 5 Torr of ^{13}CO .

the ^{13}CO pressure must be raised to approximately 400 Torr to exchange the LF band completely. After exchange, the LF band is in the same location and has the same bandwidth as the LF band present after pure ^{13}CO adsorption. The CO isotopic exchange of the LF band is reversible. These observations are in good agreement with those reported earlier by Cant and Bell (7) and Chen *et al.* (9).

A series of $^{12}\text{CO} : ^{13}\text{CO}$ coadsorption experiments were performed to determine the mode of adsorption of CO. The spectra

from the adsorption of 25:75, 50:50, and 75:25 $^{12}\text{CO} : ^{13}\text{CO}$ mixtures on reduced catalyst are given in Fig. 7. The LF band location and width vary with the ratio of $^{12}\text{CO} : ^{13}\text{CO}$. Examination of the HF band region given in Fig. 8 shows that the HF₁ band is composed of four bands at 2144, 2136, 2124, and 2095 cm^{-1} the intensities of which vary with the mixture composition. The bands at 2144 and 2095 cm^{-1} correspond to the HF₁ bands for pure ^{12}CO and pure ^{13}CO , respectively, as indicated in Table 2. Since the HF₂ bands overlap with the

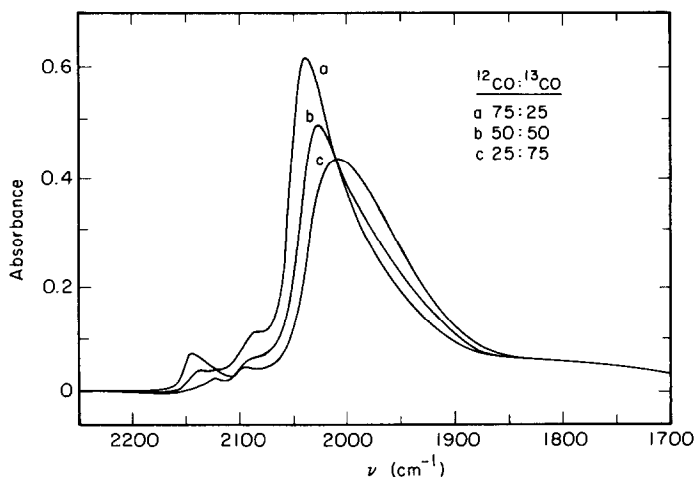


FIG. 7. Spectra of coadsorbed ^{12}CO and ^{13}CO on reduced Ru/SiO_2 .

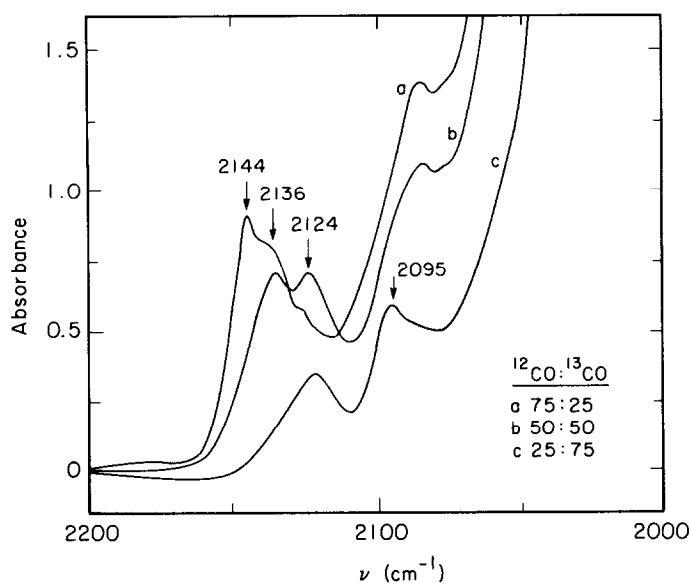


FIG. 8. Enlargement of HF band area of the spectra shown in Fig. 7.

LF band, only the HF₂ band corresponding to pure ¹²CO is distinguishable at 2082 cm⁻¹.

Figure 9 shows spectra of the oxidized catalyst following the coadsorption of ¹²CO and ¹³CO and subsequent exposure of the catalyst to ¹³CO to shift the LF band to lower frequency. Of the four bands observed, only the three highest frequency

bands are associated with the HF species, since these bands do not shift when the catalyst is exposed to ¹³CO following the coadsorption of ¹²CO and ¹³CO. The band position of the two highest frequency bands depends on the ratio of ¹²CO:¹³CO. The third band at 2029–33 cm⁻¹ corresponds to the HF₂ band of pure ¹³CO, as shown in Table 3.

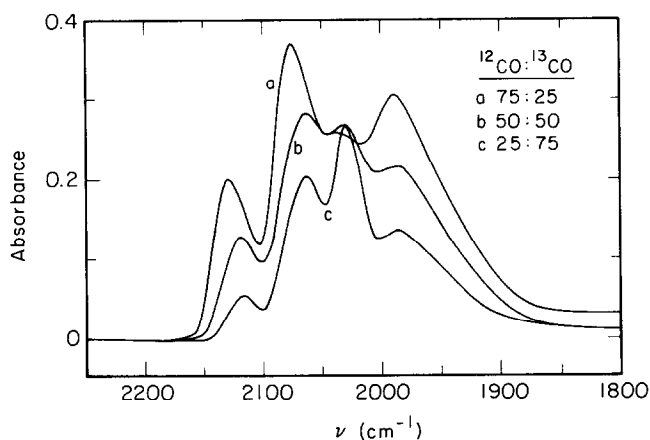


FIG. 9. Spectra of coadsorbed ¹²CO and ¹³CO on oxidized Ru/SiO₂, taken after exposure of the catalyst to a ¹³CO:¹²CO mixture and subsequent exchange of linearly adsorbed ¹²CO by exposure to ¹³CO.

TABLE 2
CO Band Positions for Mixtures of $^{12}\text{CO} : ^{13}\text{CO}$
Adsorbed on Reduced Ru/SiO₂

$^{12}\text{CO} : ^{13}\text{CO}$	$\nu_{\text{CO}} (\text{cm}^{-1})$				
		HF ₁		HF ₂	LF
100 : 0	2144	—	—	2082	2047
75 : 25	2144	2136	—	2082	2034
50 : 50	2144(sh) ^a	2136	2124	2095	2082
25 : 75	—	2136(sh)	2124	2095	2082(sh) ^a
0 : 100	—	—	—	2095	2036

^a Shoulder.

DISCUSSION

Table 4 shows that the CO vibrational frequencies observed in this study are in good agreement with those reported in previous investigations. In accordance with the literature, the LF band observed on reduced Ru/SiO₂ is assigned to linearly adsorbed CO on metallic Ru (3–8, 12–15). The upscale shift in the location of the LF band with increasing coverage, seen in Fig. 5, is due to adsorbate–adsorbate interactions, a well-documented phenomenon for CO adsorption on the surface of bulk metals (16–19). The occurrence of these interactions is further indication that the linearly adsorbed CO is on Ru particles.

The present assignment of the LF band differs from that of Chen *et al.* (9), who attributed this band to a multiple carbonyl. This assignment was based on the observation that coadsorption of ^{12}CO and ^{13}CO

produced a single asymmetric band, rather than a spectrum which is the superposition of the LF bands for ^{12}CO and ^{13}CO . While the discussion given by Chen *et al.* (9) is reasonable, the observation of only a single asymmetric band does not rule out the assignment of the LF band to linearly adsorbed CO. Theoretical analyses of coadsorbed ^{12}CO and ^{13}CO (20, 21) show that for a fixed coverage, the ^{12}CO band shifts to lower frequencies and the frequency of the ^{13}CO band shifts to higher frequencies as the percentage of ^{12}CO in the mixture decreases. It is also found that because of dipole–dipole coupling between both the in- and out-of-phase motions of neighboring adsorbed ^{12}CO and ^{13}CO , the intensity of the band for ^{12}CO is significantly larger than that for ^{13}CO projected on the basis of the isotopic ratio of the adsorbate mixture. These effects, together with line-broadening due to site heterogeneity for supported catalysts, make it difficult, in general, to resolve the two bands expected theoretically. In the present study, the FWHM of the LF peak for either pure ^{12}CO or ^{13}CO is

TABLE 4
Infrared Band Assignments for ^{12}CO Adsorbed
on Ru/SiO₂

Frequency (cm ⁻¹) reduced (oxidized)	Assignment	Adsorption site	Ref.
2150 (2135)	Linear	RuO	(3)
2080 (2080)	Linear	Ru–O	
2030 (2030)	Linear	Ru	
2140 2080 (2130)(2070)	Dicarbonyl	Ru ^{δ+}	(4)
2050 (2040)	Linear	Ru	
2050	Linear	Ru	(5)
2146 2085	Dicarbonyl	Ru	
2020	Linear	Ru	(6)
2140 2090	Not assigned		(7)
2048	Linear	Ru	
(2132)(2070)	Dicarbonyl	Ru ^{δ+}	(8)
(2020)	Linear	Ru	
2136–42 (2130)	Multicarbonyl	Ru(O, Cl, OH)	(9)
2080–85 (2078)	Linear	Ru(O, Cl, OH)	
2034–36 (2020)	Multicarbonyl	Ru	
2038	Linear	Ru	(10)
2144 2082	Tricarbonyl	Ru ²⁺	This study
(2136)(2080)	Tricarbonyl	Ru ^{δ+}	
2047 (2032)	Linear	Ru	
(2080)	Linear	Ru ^{δ+}	

TABLE 3
CO Band Positions for Mixtures of $^{12}\text{CO} : ^{13}\text{CO}$ on
Oxidized Ru/SiO₂ After ^{13}CO Exchange

$^{12}\text{CO} : ^{13}\text{CO}$	$\nu_{\text{CO}} (\text{cm}^{-1})$		
	HF ₁	HF ₂	LF
100 : 0	2136	2080	1993
75 : 25	2128	2074	1989
50 : 50	2123	2067	1985
25 : 75	2116	2062	1983
0 : 100	2087	2034	1989

50 cm⁻¹. When a 25 : 75 ¹²CO : ¹³CO mixture is adsorbed, the FWHM of the peak increases to 75 cm⁻¹ (see Fig. 7). the larger breadth of the peak is most likely due to the overlap of the peaks for the two isotopes of CO. Consequently, we may conclude that the behavior of the LF band with changing isotopic composition of the adsorbate is completely consistent with what would be expected for linearly adsorbed CO present on the surface of Ru particles.

Assignment of the HF bands has been more controversial. Brown and Gonzalez (3) have claimed that these features are attributable to linearly adsorbed CO present next to an adsorbed oxygen atom. This assignment seems unlikely for well-reduced samples. A large number of authors (4, 5, 8) have proposed a more plausible assignment, namely that the HF bands are assignable to the symmetric and asymmetric stretches of a gemdicarbonyl. Chen *et al.* (9), on the other hand, have suggested that the HF₁ band is due to a multicarbonyl, and the HF₂ band to a linear species. As will be shown below, our data for ¹²CO : ¹³CO coadsorption indicate that the best assignment of the HF bands is to tricarbonyl, rather than dicarbonyl species.

For dicarbonyl species of C_{2v} symmetry, two bands are expected corresponding to the A₁ symmetric and the B₁ asymmetric stretching modes. When a mixture of ¹²CO and ¹³CO is adsorbed, the symmetry of the dicarbonyl is lowered to C_s. The frequencies of the new stretching vibrations can be calculated from the spectra obtained using pure ¹²CO or ¹³CO, assuming a value for the bond angle (22, 23). As shown in Table 5, the assumption of a dicarbonyl species cannot account for the location of the bands observed in this study for any reasonable value of the bond angle. Only one of the bands observed upon the coadsorption of ¹²CO and ¹³CO should be located between the positions for the symmetric stretching bands of pure (¹²CO)₂ and (¹³CO)₂, and the relative intensities of the bands attributed to (¹²CO)(¹³CO) should not vary with the

TABLE 5

CO Band Positions Predicted on the Assumption that the HF Bands are Assignable to Dicarbonyl Species

	ν_{CO} (cm ⁻¹)		Bond angle (deg)
	A'	A'	
Observed	2136	2124	—
Calculated	2136	2036	90.6*
	2110	2063	87.2**

* Angle gives correct position for 2136-cm⁻¹ band.

** Angle gives highest value for lower frequency band.

ratio of adsorbed ¹²CO to ¹³CO, in contrast to what is observed experimentally (see Fig. 7).

For a tricarbonyl of local symmetry C_{3v}, two stretching vibrations of A₁ and E symmetry are expected. For a mixture of ¹²CO and ¹³CO the degenerate E mode splits into A' and A'' modes. The monosubstituted (¹²CO)₂(¹³CO) and the disubstituted (¹²CO)(¹³CO)₂ each contribute three different frequencies (two A' and one A'' mode) for a total of six bands. The relative intensity of the monosubstituted to the disubstituted species depends on the ratio of adsorbed ¹²CO to ¹³CO. The bond angle between CO molecules in the tricarbonyl and the force constants for the C–O stretching mode and the umbrella bending mode are determined from the HF band positions for pure ¹²CO and ¹³CO (22, 23). These parameters are then used to calculate the ratio of the intensities of the tricarbonyl bands and the band positions expected for the mono and disubstituted species.

As shown in Table 6, excellent agreement is observed between the calculated and the observed band positions for the high-frequency A' mode of the mono and the disubstituted tricarbonyl species. Comparison of the predicted positions of the low-frequency A' mode and of the A'' mode with experimental observation cannot be done since these bands overlap with the bands at 2082 and 2047 cm⁻¹ for pure ¹²CO.

TABLE 6

CO Band Positions Predicted on the Assumption that the HF Bands on Reduced Ru/SiO₂ are Assignable to Tricarbonyl Species

Mode	ν_{CO} (cm ⁻¹)		
	A'	A'	A''
Observed			
¹² CO : ¹³ CO = 75 : 25	2136	n.o.	n.o.
¹² CO : ¹³ CO = 25 : 75	2124	n.o.	n.o.
Calculated			
(¹² CO) ₂ (¹³ CO)	2138	2079	2043
(¹² CO)(¹³ CO) ₂	2124	2056	2034

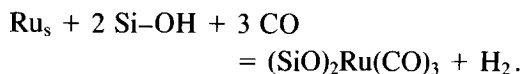
Note. Force constant for C–O bond stretching mode = 1.785×10^6 dyn/cm. Force constant for umbrella bending mode = 0.8×10^{-8} dyn/cm. Bond angle = 88.5°.

Lending further support to the assignment of the HF bands to tricarbonyl structures is the observation that the absorbances for the (¹²CO)₂(¹³CO) and (¹²CO)(¹³CO)₂ species vary as expected with the ratio of the ¹²CO : ¹³CO mixture. For the 50 : 50 ¹²CO : ¹³CO mixture, the bands at 2136 and 2124 cm⁻¹ have the same intensity. For the 75 : 25 mixture, the monosubstituted band (2136 cm⁻¹) is more intense and for the 25 : 75 mixture, the disubstituted band (2124 cm⁻¹) is more intense. The ratio of the HF₁/HF₂ band is calculated to be 0.54. This is in good agreement with the measured ratio of 0.50. The assignment of the HF bands to a multicarbonyl species is also consistent with the observation of CO/Ru adsorption ratios of greater than one for supported Ru (24–26).

The positions of the bands attributed to tricarbonyl species are very similar to those observed for ruthenium tricarbonyl complexes having the stoichiometry Ru₂(CO)₆X₄ (where X is Cl, Br, or I) (27, 28). These complexes exhibit strong absorbances at 2143–2128 and 2075–2069 cm⁻¹, and a weak absorbance at 2015–2010 cm⁻¹. The exact positions of these bands are sensitive to the electronegativity of the halogen ligands. As the electronegativity of the

halogen ligands decreases, the electron density at the Ru atoms increases. This leads to an enhancement of *d* electron back-donation into the π^* orbitals of the CO groups, as a result of which the vibrational frequencies of these groups shift down-scale. Consistent with this trend, the dominant CO frequencies in the nearly neutral tricarbonyl complexes Ru₅C(CO)₁₅ and H₂Ru₆(CO)₁₈ occur at 2066 and 2034 and 2060 and 2054 cm⁻¹, respectively (29, 30).

One may thus infer that the Ru atoms associated with the tricarbonyl species on Ru/SiO₂ bear a positive charge. This may seem surprising since thermogravimetric analysis, temperature-programmed reduction, and X-ray photoelectron spectroscopy studies have shown that Ru/SiO₂ is completely reduced by reduction in hydrogen at 573 K (31, 32). It is also noted that temperature-programmed reduction experiments carried out in the context of this study demonstrated that as little as 1% oxidation of the total Ru could readily be detected. In view of this, we propose that Ru²⁺ cations are not present in reduced catalyst but are formed by corrosive chemisorption of CO, as shown below:



Corrosive chemisorption has been shown to occur for Al₂O₃- and SiO₂-supported Rh (33, 34) and Kuznetsov *et al.* (35) have demonstrated the formation of Al–O–Ru and Si–O–Ru linkages when Ru-cluster carbonyls dispersed on Al₂O₃ are reduced at elevated temperatures. The assignment of the tricarbonyl species to isolated atoms of Ru bonded directly to SiO₂ is consistent as well with the observation that the positions of the HF bands do not shift with increasing CO adsorption. Further support for the proposed mechanism for the formation of tricarbonyl species has been obtained from temperature-programmed surface reaction studies (36). When a sample of Ru/SiO₂ containing adsorbed CO was

heated in the presence of H₂, it was observed by infrared spectroscopy that at temperatures below 400 K, the HF bands disappeared while the LF band grew in intensity. This observation can be attributed to the decomposition of tricarbonyl species and the partial readsorption of the CO onto small particles of Ru formed via the reverse of the corrosive chemisorption process.

The amounts of tricarbonyl and linearly adsorbed CO on the reduced catalyst were determined by isotopically labeling the linearly adsorbed CO and measuring the amount of labeled carbon produced during temperature-programmed reduction. Although the tricarbonyl species comprises only 10% of the spectral area, 18% of the total amount of CO is adsorbed as a tricarbonyl. The amount of CO determined by integration of CO TPD peaks assigned to the tricarbonyl and linear species is consistent with these results (36). For 18% of the CO to be adsorbed as tricarbonyls, 7% of the adsorption sites must have CO adsorbed as tricarbonyls.

Integrated-absorption coefficients for CO were calculated by dividing the integrated area of the band by the CO coverage. At saturation coverage, the integrated-absorption coefficients are estimated to be 26×10^6 and 13×10^6 cm/mol for the linear and tricarbonyl species, respectively. The magnitude of the coefficient for the linearly adsorbed CO is smaller than the value of 45×10^6 cm/mol reported previously for Ru/SiO₂ (11), but within the range 14 to 90×10^6 cm/mol reported for silica-supported Group VIII metals (37–41).

Comparison of the LF band positions for CO adsorbed on reduced and oxidized Ru/SiO₂ indicates that the C–O stretching frequency is 15 cm⁻¹ lower in the latter case. Such a difference has been observed previously (4, 9) and is best attributed to a decrease in the adsorbate interactions (17–19, 22), brought about by a decrease in the ensemble size of the linearly adsorbed CO on the oxidized catalyst.

The HF bands observed on partially oxi-

TABLE 7
CO Band Positions Predicted on the Assumption that the HF Bands on Oxidized Ru/SiO₂ are Assignable to Tricarbonyl Species

Mode	ν_{CO} (cm ⁻¹)		
	A'	A'	A''
Observed			
¹² CO : ¹³ CO = 75 : 25	2128	2074	2032
¹² CO : ¹³ CO = 25 : 75	2116	2062	2030
Calculated			
(¹² CO) ₂ (¹³ CO)	2127	2079	2042
(¹² CO)(¹³ CO) ₂	2114	2054	2033

Note. Force constant for C–O bond stretching mode = 1.785×10^{-6} dyn/cm. Force constant for CO umbrella bending mode = 0.4×10^{-8} dyn/cm. Bond angle = 88.4°.

dized Ru/SiO₂ are more difficult to assign than the HF bands observed on reduced Ru/SiO₂. In contrast to what is observed on the reduced catalyst, the ratio of the intensities of the HF₁/HF₂ bands decreases with increasing CO coverage. This behavior is not what would be expected for tricarbonyl species. As will be shown below, the HF bands are best assigned to a combination of tricarbonyl and monocarbonyl species, both present on a partially oxidized Ru surface.

Table 7 lists the HF band positions calculated for the two A' and the A'' modes for (¹²CO)₂(¹³CO) and (¹²CO)(¹³CO)₂. These calculations were made using the bond angle and force constants determined from the observed HF bands for pure ¹²CO and ¹³CO. Comparison of the calculated vibrational frequencies for tricarbonyl species containing ¹²CO and ¹³CO with those observed experimentally in coadsorption experiments support the assignment of the HF₁ band and a portion of the HF₂ band to a tricarbonyl species.

For the 75 : 25 ¹²CO : ¹³CO mixture, the most probable species is (¹²CO)₂(¹³CO). The calculated band positions for this species are 2127 and 2079 cm⁻¹, in good agreement

with the bands observed at 2128 and 2074 cm^{-1} . The predicted position of the A'' mode is 2042 cm^{-1} . This is 10 cm^{-1} higher than the observed position. The discrepancy between prediction and observation may in this case be due to the difficulty in identifying the exact position of the A'' mode since it is weak and overlaps the bands at both higher and lower frequencies. For the 25:75 $^{12}\text{CO}:^{13}\text{CO}$ mixture, the most probable species is $(^{12}\text{CO})(^{13}\text{CO})_2$. The A' modes of this species are predicted to exhibit bands at 2114 and 2054 cm^{-1} . The position of the first of these bands agrees well with that for the band observed at 2116 cm^{-1} . The observed position of the second A' mode is 2062 cm^{-1} . It should be noted, though, that the exact position of this band is difficult to establish since it resides on the rapidly rising portion of the band at 2030 cm^{-1} . The predicted position of the A'' mode is 2033 cm^{-1} , which agrees well with the experimentally observed position, 2030 cm^{-1} .

The spectra of the catalyst presented in Fig. 3 clearly show that the HF bands formed upon pulsing O_2 over a catalyst containing adsorbed CO are completely separate from the HF bands already present on the reduced surface. Such a difference in the positions of the HF band locations between oxidized and reduced catalyst has also been observed previously (3, 4, 8, 9). The observation of two sets of HF bands suggests that the tricarbonyls are adsorbed on different sites. Brown and Gonzalez (3) have proposed that the sites are differentiated by the degree of oxidation. The increase in the intensity of the bands at 2087 and 2034 cm^{-1} with increasing degree of oxidation seen in Fig. 3 is consistent with similar observations reported in the literature (3, 4, 8, 9) and gives further support to the assignment of these features to CO adsorbed on partially oxidized sites, $\text{Ru}^{\delta+}$.

The tricarbonyls on the oxidized sample are probably located on Ru particles. Pulsing oxygen over the catalyst causes the

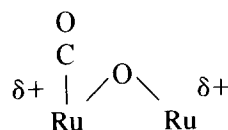
amount of linearly adsorbed CO on Ru particles to decrease significantly and leads to the formation of a tricarbonyl species on partially oxidized Ru sites. Oxidation of the Ru particles may cause a surface roughening thereby producing sites at which CO can adsorb to form tricarbonyl groups. The appearance of the HF bands on the oxidized sample at slightly lower frequencies than on reduced Ru (see Table 4) supports the proposition that the $\text{Ru}^{\delta+}$ ions reside on the oxidized surface of Ru particles. On the oxidized surface, one might envision the tricarbonyl species to be present as $(\text{RuO})_2\text{Ru}(\text{CO})_3$. In such a structure the Ru atom attached to the CO ligands should be less highly oxidized than in $(\text{SiO})_2\text{Ru}(\text{CO})_3$. Since the frequency of the HF bands in halotricarbonyl complexes is known to shift downscale with reduced positive charge on the Ru atom (27, 28), we should expect the HF bands for $(\text{RuO})_2\text{Ru}(\text{CO})_3$ to occur at lower frequencies than the corresponding bands for $(\text{SiO})_2\text{Ru}(\text{CO})_3$.

While the calculations presented in Table 7 support the assignment of the HF bands observed on oxidized Ru/SiO₂ to tricarbonyl species, the observed decrease in the ratio of the HF₁ band intensity to the HF₂ band intensity with decreasing CO coverage shown in Table 2 is inconsistent with this assignment. It is also noted the HF₂ band grows well in advance of the growth of the HF₁ band, as seen in Fig. 6.

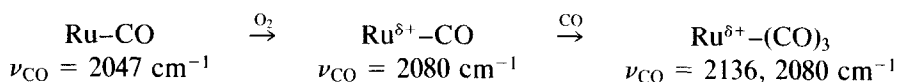
These observations can be explained by proposing the existence of a linearly adsorbed CO on $\text{Ru}^{\delta+}$ sites, which vibrates at the same frequency as the HF₂ band. The partial desorption of the tricarbonyl species leaving a linearly adsorbed CO on the partially oxidized Ru site could explain the decrease in the ratio of the HF bands with outgassing. As outgassing progresses, increasing amounts of the tricarbonyl species are converted into linearly adsorbed CO causing the intensity of the HF₂ band to increase. A similar phenomenon has been observed by Kermarec *et al.* (42) for $\text{Ni}^+(\text{CO})_2$

(2131 and 2083 cm⁻¹) which transformed into Ni⁺(CO) (2086 cm⁻¹) upon evacuation at 423 K. Evidence for the partial desorption of the tricarbonyl to form a linear CO has also been observed during temperature-programmed reduction of CO adsorbed on a reduced Ru/SiO₂ catalyst (36).

The presence of linearly adsorbed CO on Ru^{δ+} sites with a vibrational frequency equivalent to that of the HF₂ band could explain the results seen in Fig. 3. When O₂ is pulsed over reduced Ru/SiO₂ containing preadsorbed CO, the ratio of HF₁/HF₂ bands is much smaller than the expected value of 0.54 for a tricarbonyl species. Most likely, pulsing O₂ over the catalyst removes some of the linearly adsorbed CO and CO₂ and oxidizes the surface of the Ru crystallites. Some of the remaining linearly adsorbed CO is then located on Ru sites perturbed by adsorbed oxygen atoms, as shown below:



With additional pulsing of O₂, the number of Ru^{δ+} sites would be expected to increase and so would the number of CO molecules associated with these sites. This would explain why the intensity of the HF₂ band increases more rapidly with the number of O₂ pulses than does the intensity of the HF₁ band. The proposed interpretation also predicts that the adsorption of CO following the passage of O₂ pulses over the catalyst should result in the formation of tricarbonyl species and a concurrent increase in the ratio of HF₁/HF₂ up to approximately 0.5. Figure 4 shows that this is indeed what occurs. In summary, the effects of O₂ pulsing, followed by readsorption of CO, can be represented by:



CONCLUSIONS

The conclusions of this paper can be summarized as follows. On reduced Ru/SiO₂, adsorbed CO exhibits bands at 2144, 2082, and 2047 cm⁻¹. The two high-frequency bands are assigned to tricarbonyl species associated with Ru²⁺ cations bonded directly to the support by Si-O-Ru bonds. These structures are produced by corrosive chemisorption of CO on small particles of Ru. The low-frequency band is assigned to linearly adsorbed CO on reduced particles of Ru. When Ru/SiO₂ is partially oxidized, CO adsorption results in the appearance of bands at 2136, 2080, and 2032 cm⁻¹. The band at 2136 cm⁻¹ and a portion of the band at 2080 cm⁻¹ are assigned to tricarbonyl species existing on the

surface of partially oxidized Ru particles. The remainder of the band at 2080 cm⁻¹ is attributed to CO linearly adsorbed on Ru sites perturbed by adsorbed oxygen atoms. Finally, the band at 2032 cm⁻¹ is assigned to CO adsorbed on Ru sites not extensively affected by adsorbed oxygen.

ACKNOWLEDGMENTS

The authors express their appreciation to Dr. Maggy Kermarec for the helpful discussions. This work was supported in part by the Division of Chemical Sciences, Office of Basic Energy Sciences, U. S. Department of Energy, under Contract DE-AC03-76SF00098. C.L. is grateful for the support of these studies by the National Science Foundation and the Centre National de la Recherche Scientifique under Grant NSF-CNRS G05-0252. G.H.Y. acknowledges an NSF Graduate Fellowship.

REFERENCES

1. Lynds, L., *Spectrochim. Acta.* **20**, 1369 (1964).
2. Kobayashi, M., and Shirasaki, T., *J. Catal.* **28**, 289 (1973).
3. Brown, M. F., and Gonzalez, R. D., *J. Phys. Chem.* **80**, 1731 (1976).
4. Davydov, A. A., and Bell, A. T., *J. Catal.* **49**, 332 (1977).
5. Yamasaki, H., Kobori, Y., Naito, S., Onishi, T., and Tamaru, K., *J. Chem. Soc. Faraday Trans. 1* **77**, 2913 (1981).
6. Gonzalez, R. D., and Miura, H., *J. Catal.* **77**, 338 (1982).
7. Cant, N. W., and Bell, A. T., *J. Catal.* **73**, 257 (1982).
8. Kiss, J. T., and Gonzalez, R. D., *J. Phys. Chem.* **88**, 892 (1984).
9. Chen, H.-W., Zhong, Z., and White, J. M., *J. Catal.* **90**, 119 (1984).
10. McClory, M. M., and Gonzalez, R. D., *J. Catal.* **89**, 392 (1984).
11. Winslow, P., and Bell, A. T., *J. Catal.* **86**, 158 (1984).
12. Thomas, G. E., and Weinberg, W. H., *J. Chem. Phys.* **70**, 1437 (1979).
13. Pfnur, H., Menzel, D., Hoffmann, F. M., Ortega, A., and Bradshaw, A. M., *Surf. Sci.* **93**, 431 (1980).
14. Hoffmann, P., and Menzel, D., *Surf. Sci.* **161**, 303 (1985).
15. Madey, T. E., *Surf. Sci.* **79**, 575 (1979).
16. Hammaker, R. M., Francis, S. A., and Eischens, R. P., *Spectrochim. Acta* **21**, 1295 (1965).
17. Primet, M., *J. Catal.* **88**, 273 (1984).
18. Blyholder, G. J., *J. Phys. Chem.* **68**, 2772 (1964).
19. Weaire, D., *Surf. Sci.* **103**, L115 (1981).
20. Hammaker, R. M., Francis, S. A., and Eischens, R. P., *Spectrochim. Acta* **21**, 1309 (1965).
21. Hoffmann, F. M., *Surf. Sci. Rep.* **3**, 107 (1983).
22. Bratermann, P. S., "Metal Carbonyl Spectra," 1st ed. Academic Press, New York/London, 1975.
23. Gelin, P., Coudurier, G., Ben Taarit, Y., and Nacache, C., *J. Catal.* **70**, 32 (1981).
24. Kobayashi, M., and Shirasaki, T., *J. Catal.* **32**, 254 (1974).
25. Okuhara, T., Kimura, T., Kobayashi, K., Misono, M., and Yoneda, Y., *Bull. Chem. Soc. Japan* **57**, 938 (1984).
26. Dalla Betta, R. A., *J. Phys. Chem.* **79**, 2519 (1975).
27. Benedetti, E., Braca, G., Sbrana, G., Salvetti, F., and Grassi, B., *J. Organomet. Chem.* **37**, 361 (1972).
28. Johnson, B. F., Johnston, R. D., Josty, P. L., Lewis, J., and Williams, G., *Nature (London)*, 902 (1967).
29. Kristoff, J. S., and Shriver, D. F., *Inorg. Chem.* **13**, 499 (1974).
30. Churchill, M. R., Wormald, J., Knight, J., and Mays, M. J., *J. Amer. Chem. Soc.* **93**, 3073 (1971).
31. Bossi, A., Garbassi, F., Orlandi, A., Petrini, G., and Zanderighi, L., *Stud. Surf. Sci. Catal.* **3**, 405 (1978).
32. Blanchard, G., Charcosset, H., Chenebauz, M. T., and Primet, M., *Stud. Surf. Sci. Catal.* **3**, 197 (1978).
33. Van't Bilk, H. F., Van Zon, J. B. A. D., Huizinga, T., Vis, J. C., Konigsberger, D. C., and Prins, R., *J. Chem. Phys.* **87**, 2264 (1983).
34. Basu, P., Panayatov, D., and Yates, J. T., Jr., *J. Amer. Chem. Soc.* **110**, 2074 (1988).
35. Kuznetsov, V. L., and Bell, A. T., *J. Catal.* **65**, 374 (1980).
36. Yokomizo, G. H., Louis, C., and Bell, A. T., *J. Catal.* **120**, 15 (1989).
37. Seanor, D. A., and Amberg, C. H., *J. Chem. Phys.* **42**, 2967 (1965).
38. Duncan, T. M., Yates, J. T., Jr., and Vaughn, R. W., *J. Chem. Phys.* **73**, 975 (1980).
39. Vannice, M. A., and Twu, C. C., *J. Chem. Phys.* **75**, 5944 (1981).
40. Vannice, M. A., and Wang, S.-Y., *J. Phys. Chem.* **55**, 2543 (1981).
41. Cant, N. W., and Donaldson, R. A., *J. Catal.* **78**, 461 (1982).
42. Kermarec, M., Delafosse, D., and Che, M., *J. Chem. Soc. Chem. Commun.*, 411 (1983).